

# Parametric study of transition fluidic control in a dual-bell nozzle

*Andrea Ferrero\**, *Antonietta Conte\**, *Emanuele Martelli†*, *Francesco Nasuti††* and *Dario Pastrone\**

*\*Politecnico di Torino*

*Corso Duca degli Abruzzi 24, Torino, Italy*

*†Università della Campania Luigi Vanvitelli*

*Via Roma 29, Aversa, Italy*

*††Sapienza Università di Roma*

*Via Eudossiana 18, Roma, Italy*

## Abstract

The dual-bell nozzle is a promising concept for improving the performance of first-stage liquid rocket engines. It is characterised by the presence of two altitude-dependent working modes which allow to reduce non-adaptation losses. However, the transition between the two working modes usually takes place prematurely and dangerous side loads might be observed. In this work, fluidic control is investigated as a potential method to delay the transition and limit the risk of side loads. An Ariane 5-like launcher configuration with a dual-bell nozzle in the core engine is considered. First, a parametric optimisation is performed to identify the dual-bell geometry that maximises the payload mass delivered into geostationary transfer: a preliminary model is adopted to describe the dual-bell mode transition and a fast and reliable in-house trajectory optimisation code is used to optimise the ascent trajectory. The flow field in the optimal geometry is then investigated by CFD simulations to verify the effectiveness of fluidic control. Finally, the CFD study results are used to model the dual-bell mode transition and trajectory optimisation is performed again. The proposed solution is characterised by a large payload gain with respect to the reference launcher. Fluidic control significantly reduces side loads which can arise during transition.

## 1. Introduction

Rocket engines used in the first stage of space launchers work from sea-level to almost vacuum conditions. An example is represented by the Vulcain 2 liquid rocket engine used in the Ariane 5 launcher. The area ratio of its nozzle is limited by the necessity to avoid uncontrolled separation and dangerous side loads at lift-off. This limitation has a significant impact on the engine's performance when high altitudes are reached.

In order to avoid such limitations of classical bell nozzles, several alternatives have been proposed and studied [4, 5, 11, 12, 15, 18, 19]. Among them, the dual-bell nozzle represents a promising solution because of its effectiveness and the minor changes it requires with respect to conventional nozzles. The basic idea is to consider a bell shaped nozzle connected to a bell shaped extension by means of an inflection: the discontinuity in the contour slope allows anchoring the separation line and avoiding side loads at low altitudes. When the external pressure reduces below a threshold value, transition occurs and full flow working conditions are obtained. The presence of these two working modes significantly improves the specific impulse, which strongly affects launcher performance especially at higher altitudes where actual payload mass fraction is larger. However, there are two possible drawbacks related to the transition process. The first one is associated to an early transition to the high-altitude working mode which would limit the performance gain. This anticipated transition is caused by a value of the static pressure in the separated-flow region in the second bell which is lower than the ambient pressure. The second one is far more critical as it is a possible obstacle to the real implementation of this solution: significant side loads can be observed during the transition process [6]. Several strategies have been investigated to control the transition, such as fluidic control [10, 28, 29], film cooling [17, 23, 26], and mixture ratio variation [26]. Fluidic control is a promising strategy which consists in injecting fluid through a slot near the inflection point; the injected fluid represents an obstacle to the supersonic flow and allows control of the position of the separation line.

In this work, a configuration inspired by the Ariane 5 launcher with a dual-bell in the core engine is studied, and fluidic control is investigated as a potential strategy to delay the transition and limit the magnitude of side loads.

## TRANSITION CONTROL IN A DUAL-BELL NOZZLE

First of all, a preliminary optimisation study is performed on the dual-bell geometry and on the launcher trajectory to maximise the payload gain. This preliminary optimisation is based on the assumption that fluidic control is able to increase the transitional nozzle pressure ratio (NPR) to the optimal value corresponding to the best performance.

As a second step, the flow field inside the optimal dual-bell nozzle is investigated by CFD simulations for several values of NPR to verify the fluidic control effectiveness. The CFD study enabled the determination in more detail of the fluidic control requirements in terms of mass flow rate and activation time. These data are then used to update the optimal solution.

## 2. Optimisation

The present work analyses the payload optimisation for an Ariane 5-like launcher in which the Vulcain 2 nozzle is substituted by a dual-bell nozzle with a constant pressure extension. This study is made in analogy with [27] where the impact of the dual-bell nozzle on the payload mass delivered into a reference geosynchronous transfer orbit (GTO) by Ariane 5 ECA is evaluated. Stark et al. [27] investigated several dual-bell nozzle contours with constant pressure extension by changing the area ratio of the first bell ( $\epsilon_1$ ) and the inflection angle ( $\alpha$ ). The best solution was identified using both an analytical approach based on the ideal rocket velocity increment and a trajectory optimisation procedure. They showed that a significant payload gain can be obtained. In the present work the goal is still to maximise the payload mass inserted into a reference GTO launching from Kourou, but a controlled dual-bell mode transition is considered. Two free parameters are considered to define the dual-bell nozzle geometry: the inflection angle ( $\alpha$ ) and the truncation percentage ( $\lambda$ ) of the second bell. The reference contour for the second bell is a constant pressure contour ending when it reaches the direction of nozzle axis. The actual bell is obtained by truncating the second bell contour to a certain fraction ( $\lambda$ ) with respect to the reference one. It is worth noting that the area ratio of the first bell is kept fixed ( $\epsilon_1 = 50$ ) according to the best configuration reported in [27], whereas the introduction of the truncation percentage ( $\lambda$ ) of the second bell allows for beneficial nozzle weight reduction.

The design parameters are allowed to assume values in the intervals  $7^\circ < \alpha < 17^\circ$  and  $0.5 < \lambda < 1$ , but two size constraints are imposed on the engine length ( $L < 4.5$  m) and maximum expansion ratio ( $\epsilon_2 < 150$ ). These values are in line with the limitations chosen by [27] which are determined by the launch pad margins. For each nozzle geometry, the ascent trajectory is optimised using a fast and efficient in-house solver based on the optimal control theory [7] which was presented and used in [5, 11].

The nozzle mass is estimated by assuming a uniform weight distribution ( $35 \text{ kg/m}^2$ ) evaluated from the data reported by [27]. The thrust contribution of the base is evaluated by performing an inviscid CFD simulation. The aspiration drag in the low altitude working condition is assumed as negligible, while the thrust contribution provided by the extension in the high-altitude working mode is easily computed by considering a Prandtl-Meyer expansion centred at the inflection point.

The simulations are performed assuming that the secondary injection is activated ( $NPR_{ON}$ ) when the natural transitional NPR is reached. The natural transitional NPR is estimated by means of the Schmucker criterion [25] in this preliminary evaluation. The secondary injection is deactivated ( $NPR_{OFF}$ ) when the launcher reaches the optimal transitional NPR which guarantees the best performance of the dual-bell nozzle. The optimal NPR is determined by the condition in which the dual-bell provides the same thrust in both working modes.

In this parametric analysis, the mass flow rate used for the fluidic control is preliminary assumed to be 3 % of the main combustion chamber mass flow. A mass budget of 500 kg is allocated for the fluidic control system, including both dry masses and the control fluid mass which is reduced in time according to the prescribed secondary flow mass flow rate. The results of this preliminary parametric study are reported in Figure 1 which shows the payload gain as a function of the design parameters  $\alpha$  and  $\lambda$ . The plot also shows the constraint limits: feasible solutions are localised below both curves. To accurately determine the constrained optimal point, an optimisation procedure is implemented in Matlab by using the active-set algorithm for constrained optimisation. The optimal solution is characterised by the parameters reported in Table 1.

## 3. Fluidic control of transition

The flow field inside the optimal dual-bell nozzle is numerically studied to determine the required properties of the secondary injection at optimal NPR. Specifically, the mass flow needed to control the transition, the value of the natural transitional NPR (which determines  $NPR_{ON}$ ) and the maximum NPR that can be obtained using the fluidic control (i.e maximum allowable  $NPR_{OFF}$ ), are searched for. A preliminary parametric study showed that it is not possible to

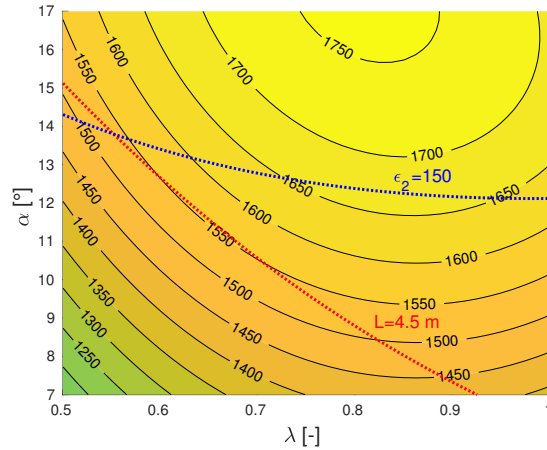


Figure 1: Optimisation results: payload gain (kg) as a function of design parameters. Red and blue dotted curves represents nozzle length constraint ( $L < 4.5$  m) and maximum expansion ratio constraint ( $\epsilon_2 < 150$ ) respectively

Table 1: Optimal solution obtained by the preliminary study

$\alpha$ [°]	11.46
$\lambda$ [-]	0.6552
$h_{ON}$ [km]	5
$h_{OFF}$ [km]	13
$NPR_{ON}$ [-]	222
$NPR_{OFF}$ [-]	775
$\dot{m}_i/\dot{m}$ [-]	0.03
$m_{CS}$ [kg]	500
$\Delta m_{PL}$ [kg]	1556

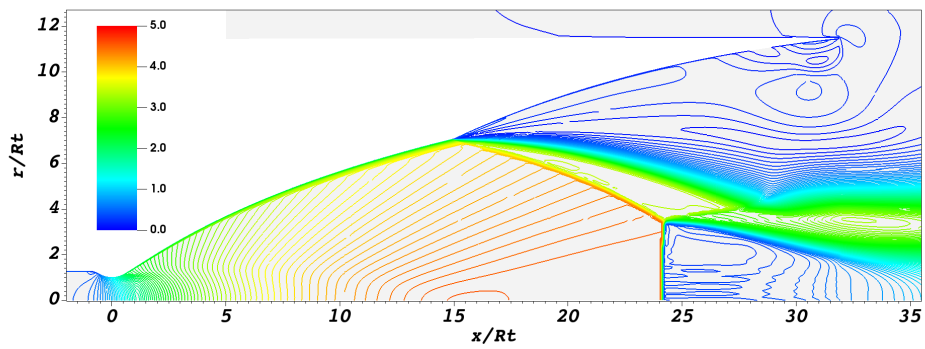
increase the transitional NPR up to the optimal value ( $NPR=775$ ) [8]. However, the impact of the transitional NPR on the final payload is relatively small because the transition takes place when the boosters are still active. This fact suggests the choice of an alternative scenario in which the secondary injection is used to increase the transitional NPR to mitigate the premature transition (even if the optimal transitional NPR is not reached) and, moreover, to minimise the occurrence of side loads by keeping the separation line fixed at the inflection point (where the wall pressure gradient is very large). In such a way, the transition takes place impulsively by deactivating the secondary injection.

The simulations are carried out by numerically solving the Reynolds-averaged Navier-Stokes (RANS) equations based on an adaptive version of the Spalart and Allmaras model [1], which applies a compressibility correction [21] only in the shear layer and has no effect on the production term in the boundary layer [10]. The flow is assumed to be 2-D axisymmetric, steady, and compressible. An ideal gas with a constant specific heat ratio  $\gamma = 1.14$  is considered. Viscosity is evaluated by using the Sutherland's law for water which is the main combustion product. The nozzle wall is considered adiabatic. A parallel implicit code based on an unstructured finite-volume discretization of the domain was adopted to integrate the governing equations [10]. The mesh size was determined by a previous study [8]. The spatial discretisation is accurate to the second order and the reconstruction required by convective fluxes is limited using the Barth-Jespersen technique [3], whereas the gradient required by diffusive fluxes and source terms is computed using the weighted least square method. Convective fluxes are evaluated using a hybrid solver [9] that combines Flux Difference Splitting [20, 22] and the local Lax-Friedrichs (or Rusanov) flux [24]. The computational domain is discretized using the Frontal-Delaunay for quads algorithm by the Gmsh tool [14]. The unstructured grid is managed in the parallel MPI environment via the DMplex class [16] provided by the PETSc library [2].

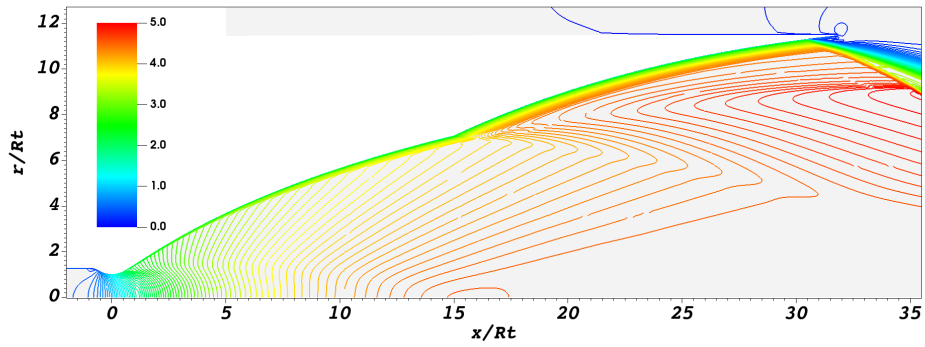
The flow field is investigated first without introducing the secondary injection. The Mach number contour lines at  $NPR=115$  and  $NPR=185$  are reported in Figure 2 which shows the low-altitude and the high-altitude working modes. The wall pressure distribution is reported in Figure 3: the plot shows that the RANS simulations predict the natural transition in the range  $170 < NPR < 175$ .

However, it is possible to observe a significant displacement of the separation line within the inflection region [19] when the NPR is increased from  $NPR=115$  to  $NPR=170$ . In particular, the wall pressure gradient at the separation location can assume relatively small values when the NPRs increases from the sea-level condition to the

## TRANSITION CONTROL IN A DUAL-BELL NOZZLE



(a)



(b)

Figure 2: Mach number contour lines at NPR=115 (a) and NPR=185 (b) without control.

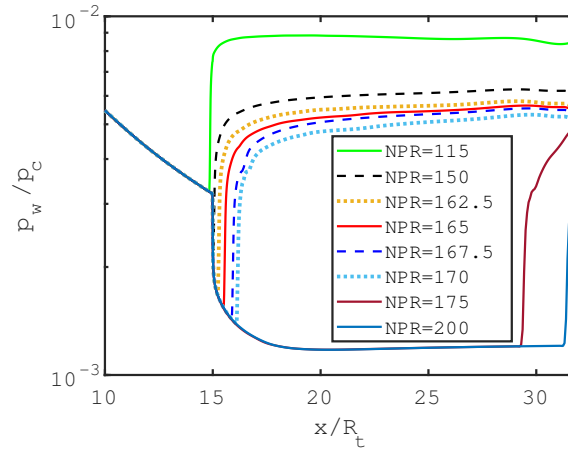


Figure 3: Wall pressure distribution in the optimized dual-bell nozzle for  $115 < \text{NPR} < 175$  without control.

transitional NPR. According to [25], the magnitude of the side loads increases when the wall pressure gradient upstream of the separation point decreases: this means that significant side loads could be obtained if natural transition occurs [13]. In particular, the magnitude of the nondimensional side loads can be estimated according to [25] as:

$$\Phi = \frac{r_s}{R_T} \frac{p_s}{p_c} \left( 1 - \frac{p_s}{p_a} \right) \frac{1}{\frac{dp_s/p_c}{d(l/R_t)}} \frac{1}{1 - \frac{1 + \frac{\gamma-1}{2} M_s^2}{(1.88 M_s - 1) M_i} \frac{1.2}{\gamma}} \quad (1)$$

where  $r_s$ ,  $p_s$ ,  $\frac{dp_s/p_c}{d(l/R_t)}$  and  $M_s$  represent radius, wall pressure, normalized wall pressure gradient and wall isentropic Mach number at the separation point, respectively.

A second set of simulations is performed by activating the secondary injection to delay the transition. The secondary flow is radially injected at  $x/R_t = 16$  through a 1 cm slot. The total temperature and total pressure of the injection are assumed to be equal to 300 K and 1.96 bar, respectively. The flow through the injection slot is assumed to be supersonic ( $M = 2$ ). A discussion on the use of sonic or supersonic injection is reported in [8]. The effect induced by the secondary injection is evident in Figure 4 which shows the Mach number contour lines at  $\text{NPR}=200$  for the uncontrolled and controlled configurations: the uncontrolled flow is reattached while the flow with the secondary injection is still separated. The plot shows that the secondary jet acts as an obstacle for the supersonic flow, inducing a fluidic ramp and keeping the separation fixed at the inflection point.

More details can be deduced from the wall pressure distribution which is reported in Figure 5 for several values of NPR: the plot shows that the separation line remains confined close to the inflection point for  $\text{NPR} < 205$ . This represents a significant extension of the transitional NPR with respect to the result obtained for the uncontrolled flow ( $\text{NPR} < 175$ ). The effects of the secondary injection on the location of the separation line for several values of NPR is reported in Figure 6. It is evident how the separation line remains well anchored at the inflection point for a longer range of nozzle pressure ratios. Finally, the wall pressure gradient upstream of the separation line is systematically larger in the controlled flow with respect to the values observed for the natural transition. This means that in the controlled flow the expected magnitude of the side loads is expected to be reduced with respect to the uncontrolled configuration, according to the correlation proposed by [25]. This is clarified by the plot reported in Figure 7.

#### 4. Corrections to the optimal solution

The CFD study enabled a more complete understanding of the control system requirements. In particular, the side loads estimation reported in Figure 7 suggests the following choice:  $\text{NPR}_{ON} = 160$  and  $\text{NPR}_{OFF} = 200$ . In this manner, the control system is activated before significant side loads are observed, and it is deactivated at a NPR significantly higher than the natural transitional NPR, resulting in a rapid transition to full flow working conditions.

The new  $\text{NPR}_{ON}$ ,  $\text{NPR}_{OFF}$  and  $\dot{m}_i = 0.0315\dot{m}$  are then used to run an updated trajectory optimisation analysis. A first optimal configuration is obtained by setting  $m_{CS} = 500$  kg. Even if  $\text{NPR}_{OFF}$  was decreased from the optimal value (775) to a significantly lower but feasible value (200) the payload gain remains high ( $\Delta m_{PL} = 1457$  kg). In this new configuration, the fluidic control system remains active for approximately 10 seconds when the launcher increases its altitude from 2 km to 4 km. The mass of the fluid injected in this time interval is relatively small (70 kg), especially if

## TRANSITION CONTROL IN A DUAL-BELL NOZZLE

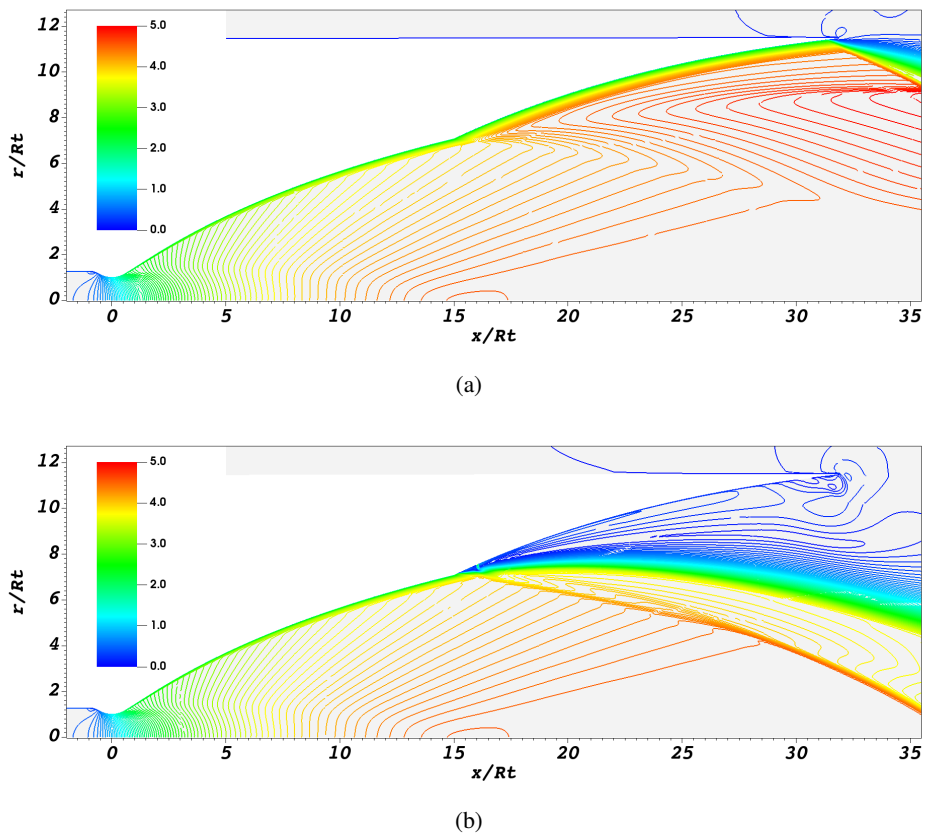


Figure 4: Mach number contour lines at NPR=200 without control (a) and with control (b).

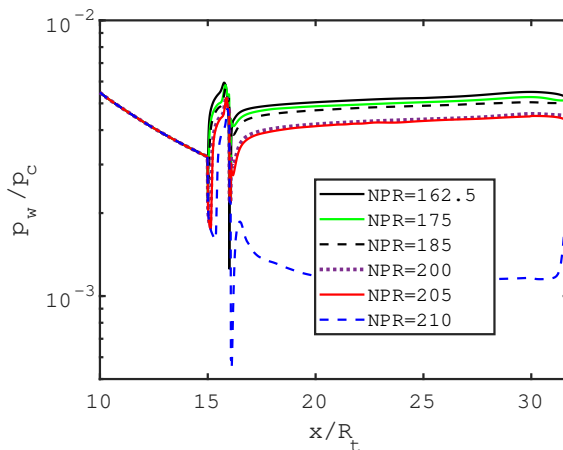


Figure 5: Wall pressure distribution in the optimized dual-bell nozzle for  $175 < \text{NPR} < 220$  with secondary injection.

compared to the mass injected in the optimal configuration obtained by the preliminary study (230 kg). For this reason, a further trajectory optimisation was performed by reducing the mass budget allocated for the fluidic control system to  $m_{CS}=400$  kg. This has a positive effect on the payload, which is increased further ( $\Delta m_{PL} = 1497$  kg). Finally, in Figure 8 a plot of the altitude as a function of time is reported and the key points of the mission are highlighted.

## TRANSITION CONTROL IN A DUAL-BELL NOZZLE

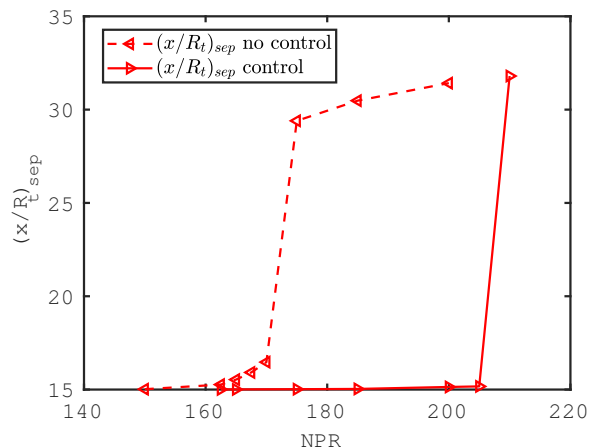


Figure 6: Separation location for uncontrolled and controlled flow.

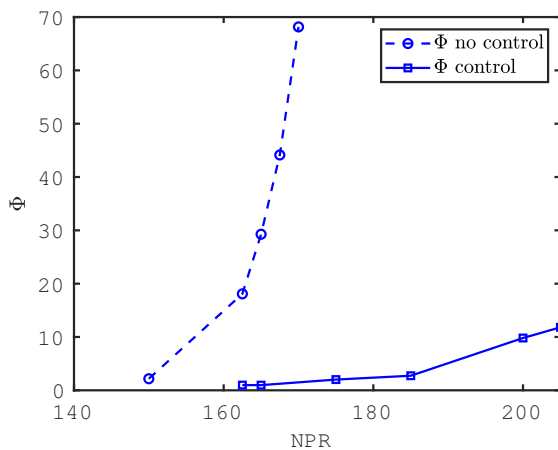


Figure 7: Nondimensional side loads for uncontrolled and controlled flow.

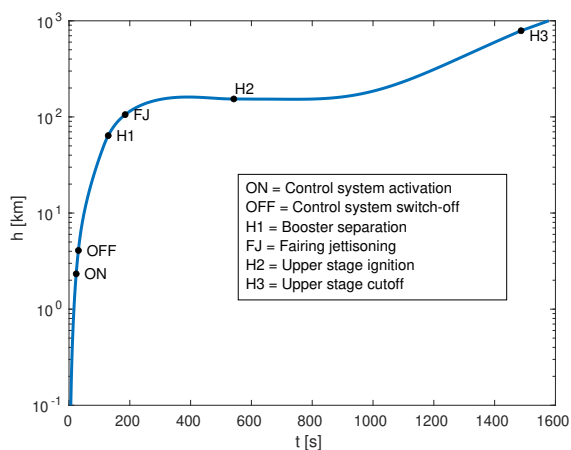


Figure 8: Optimal trajectory with controlled transition.

## 5. Conclusions

The benefits related to the use of the dual-bell nozzle in the core engine of the Ariane 5 like launcher are investigated by means of a parametric study in which both the nozzle geometry and the ascent trajectory were optimised. There

## TRANSITION CONTROL IN A DUAL-BELL NOZZLE

are two main results in the present work. First of all, the study showed that significant payload gains can be obtained (approximately 1.5 ton in GTO for an Ariane-5 like launcher). The second result is related to the effectiveness of a secondary injection in controlling the separation position during the ascent: this is important because side loads can be a critical issue in the real application of a dual-bell. In particular, the simulations highlighted once more that, in the uncontrolled flow, the separation line moves in the inflection region where it is known that significant side loads can be generated. The use of a secondary injection performed downstream of the inflection point consent to significantly limit the displacement of the separation line, which remains in regions characterised by a large wall pressure gradient until the injection is deactivated. This feature could be very useful to synchronise the transition in a full-liquid configuration with multiple dual-bell nozzles. The CFD simulations and the reduced activation time suggested that the control could be realised by the injection of a cold gas stored inside a dedicated tank. Alternative sources for the injected fluid will be investigated in the future, as well as, the effectiveness of fluidic control in the presence of reacting flows.

## References

- [1] Steven R Allmaras and Forrester T Johnson. Modifications and clarifications for the implementation of the spallart-allmaras turbulence model. In *Seventh international conference on computational fluid dynamics (ICCFD7)*, pages 1–11, 2012.
- [2] Satish Balay, Shrirang Abhyankar, Mark Adams, Jed Brown, Peter Brune, Kris Buschelman, Lisandro Dalcin, Alp Dener, Victor Eijkhout, W Gropp, et al. *Petsc users manual*. 2019.
- [3] Timothy Barth and Dennis Jespersen. The design and application of upwind schemes on unstructured meshes. In *27th Aerospace sciences meeting*, page 366, 1989.
- [4] Luca Boccaletto and Jean-Paul Dussauge. High-performance rocket nozzle concept. *Journal of Propulsion and Power*, 26(5):969–979, 2010.
- [5] Lorenzo Casalino, Dario Pastrone, and Francesco Simeoni. Effects of limitation of nozzle flow separation on launcher performance. *Journal of Propulsion and Power*, 29(4):849–854, 2013.
- [6] M Cimini, E Martelli, and M Bernardini. Numerical analysis of side-loads reduction in a sub-scale dual-bell rocket nozzle. *Flow, Turbulence and Combustion*, pages 1–24, 2021.
- [7] Guido Colasurdo and Dario Pastrone. Indirect optimization method for impulsive transfers. In *Astrodynamic Conference*, page 3762, August 1994.
- [8] Andrea Ferrero, Antonietta Conte, Emanuele Martelli, Francesco Nasuti, and Dario Pastrone. Dual-bell nozzle for space launchers with fluidic control of transition. In *AIAA Propulsion and Energy 2021 Forum*, page 3586, 2021.
- [9] Andrea Ferrero and Domenic D’Ambrosio. A hybrid numerical flux for supersonic flows with application to rocket nozzles. *Advances in Aircraft and Spacecraft Science*, 7(5):387–404, 2020.
- [10] Andrea Ferrero, Emanuele Martelli, Francesco Nasuti, and Dario Pastrone. Fluidic control of transition in a dual-bell nozzle. In *AIAA Propulsion and Energy 2020 Forum*, page 3788, 2020.
- [11] Andrea Ferrero and Dario Pastrone. Plasma actuator–assisted rocket nozzle for improved launcher performance. *AIAA Journal*, 57(4):1348–1354, 2019.
- [12] Manuel Frey and Gerald Hagemann. Critical assessment of dual-bell nozzles. *Journal of propulsion and power*, 15(1):137–143, 1999.
- [13] Chloe Genin and Ralf H Stark. Side loads in subscale dual bell nozzles. *Journal of Propulsion and Power*, 27(4):828–837, 2011.
- [14] Christophe Geuzaine and Jean-François Remacle. Gmsh: A 3-d finite element mesh generator with built-in pre- and post-processing facilities. *International journal for numerical methods in engineering*, 79(11):1309–1331, 2009.
- [15] Gerald Hagemann, Hans Immich, Thong Van Nguyen, and Gennady E Dumnov. Advanced rocket nozzles. *Journal of Propulsion and Power*, 14(5):620–634, 1998.

- [16] Michael Lange, Matthew G Knepley, and Gerard J Gorman. Flexible, scalable mesh and data management using petsc dmpex. In *Proceedings of the 3rd International Conference on Exascale Applications and Software*, pages 71–76. University of Edinburgh, 2015.
- [17] Emanuele Martelli, Francesco Nasuti, and Marcello Onofri. Film cooling effect on dual-bell nozzle flow transition. In *45th AIAA/ASME/SAE/ASEE Joint Propulsion Conference & Exhibit*, page 4953, 2009.
- [18] Francesco Nasuti and Marcello Onofri. Theoretical analysis and engineering modeling of flowfields in clustered module plug nozzles. *Journal of Propulsion and Power*, 15(4):544–551, 1999.
- [19] Francesco Nasuti, Marcello Onofri, and Emanuele Martelli. Role of wall shape on the transition in axisymmetric dual-bell nozzles. *Journal of propulsion and power*, 21(2):243–250, 2005.
- [20] Stanley Osher and Fred Solomon. Upwind difference schemes for hyperbolic systems of conservation laws. *Mathematics of computation*, 38(158):339–374, 1982.
- [21] Renato Paciorri and Filippo Sabetta. Compressibility correction for the spalart-allmaras model in free-shear flows. *Journal of Spacecraft and Rockets*, 40(3):326–331, 2003.
- [22] Maurizio Pandolfi. A contribution to the numerical prediction of unsteady flows. *AIAA journal*, 22(5):602–610, 1984.
- [23] Dzianis Proschanka, Koichi Yonezawa, Hidekazu Koga, Yoshinobu Tsujimoto, Tatsuya Kimura, and Kazuhiko Yokota. Control of operation mode transition in dual-bell nozzles with film cooling. *Journal of Propulsion and Power*, 28(3):517–529, 2012.
- [24] Vladimir Vasilevich Rusanov. The calculation of the interaction of non-stationary shock waves and obstacles. *USSR Computational Mathematics and Mathematical Physics*, 1(2):304–320, 1962.
- [25] R. H. Schmucker. Flow process in overexpanded chemical rocket nozzles. part 1: Flow separation. *NASA TM-77396*, January 1984.
- [26] Dirk Schneider, Ralf Stark, Chloé Génin, Michael Oswald, and Konstantin Kostyrkin. Active control of dual-bell nozzle operation mode transition by film cooling and mixture ratio variation. *Journal of Propulsion and Power*, 36(1):47–58, 2020.
- [27] Ralf Stark, Chloé Génin, Dirk Schneider, and Christian Fromm. Ariane 5 performance optimization using dual-bell nozzle extension. *Journal of Spacecraft and Rockets*, 53(4):743–750, 2016.
- [28] Takeo Tomita, Mamoru Takahashi, and Masaki Sasaki. Control of transition between two working modes of a dual-bell nozzle by gas injection. In *45th AIAA/ASME/SAE/ASEE Joint Propulsion Conference & Exhibit*, page 4952, 2009.
- [29] Vladeta Zmijanovic, Luc Leger, Mohamed Sellam, and Amer Chpoun. Assessment of transition regimes in a dual-bell nozzle and possibility of active fluidic control. *Aerospace Science and Technology*, 82:1–8, 2018.